



## Building a Hofmeister-like series for the maximum in density temperature of aqueous electrolyte solutions



F. Gámez<sup>a</sup>, L.F. Sedano<sup>a</sup>, S. Blazquez<sup>a</sup>, J. Troncoso<sup>b</sup>, C. Vega<sup>a,\*</sup>

<sup>a</sup> Depto. Química Física I, Fac. Ciencias Químicas, Universidad Complutense de Madrid, 28040 Madrid, Spain

<sup>b</sup> Departamento de Física Aplicada, Universidade de Vigo, Escola de Enxeñaría Aeronáutica e do Espazo, E 32004 Ourense, Spain

### ARTICLE INFO

#### Article history:

Received 11 November 2022

Revised 10 January 2023

Accepted 8 February 2023

Available online 13 February 2023

#### Keywords:

electrolytes

Maximum in density

Despretz law

Experiments

Madrid-2019 force field

Hofmeister series

### ABSTRACT

The temperature of the maximum in density (TMD) at room pressure is experimentally evaluated for aqueous solutions of a set of halides containing  $F^-$ ,  $Cl^-$ ,  $Br^-$ ,  $I^-$ ,  $Li^+$ ,  $Na^+$ ,  $K^+$ ,  $Rb^+$ ,  $Cs^+$  and  $Mg^{2+}$  at a 1 m concentration. The measurements were performed by monitoring the density-temperature profiles and tracking the temperature-dependent position of the meniscus, in a capillary glass tube. Adding salts diminishes the TMD of the solutions with respect to pure water, being the magnitude of the change dependent on the nature of the electrolyte. The experimental values of the shift in the TMD can be split into individual ion contributions. From this information we were able to establish a rank of ions (i.e., a Hofmeister-like series) according to their efficiency in shifting down the TMD. The experimental results are also compared to simulation values obtained via Molecular Dynamics using the Madrid-2019 force field that assigns non-integer charges for the ions and is parametrized for the TIP4P/2005 water model. Finally, since the TMD is a fingerprint property of water, we will discuss the impact of ions on this maximum in relation with the way different ions modify the structure of water.

© 2023 The Author(s). Published by Elsevier B.V.

## 1. Introduction

The increase in the tetrahedral order of liquid water upon cooling might be behind the anomalous behavior found for many of its thermodynamic properties. Among them, the existence of a maximum in density when cooled at constant pressure is probably the most important one. At room pressure, the maximum in density occurs at a temperature of  $\sim 4^\circ C$  [1]. This temperature is called the temperature of the maximum in density (TMD), whose origin is hypothesised to rely on an experimentally elusive high-to-low density liquid-liquid transition [2–10] that has been demonstrated for some potential models of water having two length scales [11–14].

It is well known that ions modify the structure of water as it has been pointed out by many authors [15–24]. However, measuring the structural changes of water in the presence of electrolytes constitutes an experimental challenge. Taking into account that the temperature at which the maximum in density occurs is somehow a reflection of the subtle balance between tetrahedral ordering and packing, one would expect that its experimental determination could provide some indirect information about structural changes

due to the addition of ions to water. Electrolytes and in fact, most of the water-soluble substances shift the maximum in density to lower temperatures [25–28], with a few remarkable anomalies found for some alcohols [29–32]. Although the experimental determination of the TMD is rather straightforward, somewhat surprisingly, experiments regarding the TMD of electrolyte solutions were notably intense only up to 1925 [33–36,28]. After decades of drought in the field, with only some exceptions [37–40], the interest in this topic has increased in recent years [41–44], since electrolyte solutions at low temperatures have been proposed as a possible route to explore deeply supercooled water, in which homogeneous nucleation is partly hindered [45], hence facilitating the experimental access to the liquid-liquid transition [43].

Regarding the local structure of water around ions, experimental and computational efforts have been directed to unravel whether or not the effects of the ions would spread beyond the first solvation shell [46–48,17]. However, it is timely to mention the discrepancies found in the literature concerning the definitions of "structure-maker" or "structure-breaker" for ions [49,17,50]. Despite the TMD is intimately related to the structure of water [51], these concepts must be dealt with care, since no clear definition has been agreed upon. First of all, these terms can be more or less defined as the capacity of ions of enhancing (structure-makers) or destroying/distorting (structure-breakers) hydrogen bonding networks in water. Nevertheless, there are many variables

\* Corresponding author.

E-mail address: [cvega@quim.ucm.es](mailto:cvega@quim.ucm.es) (C. Vega).

to stipulate regarding this matter, such as the concentration of electrolytes in the solution or whether the structure of water refers to all the water molecules in solution or only to those beyond the solvation shell(s) (the so-called "free water"). Within the first solvation shell of most ions, some hydrogen bonds are broken because the electrostatic interactions overcome the directional H-bonding [52,20]. This is not the case for certain hydrophobic ions such as  $\text{Cs}^+$ , which induces water molecules to form ice-like cages [53,54]; or  $\text{F}^-$ , which is known to engage in H-bond networks within the water molecules in the first solvation shell [55]. Thus, it would be reasonable to conceive the structure-making/breaking concepts as how they affect the structure of water regarding H-bonding beyond the first solvation shell. Secondly, the terms structure-makers/breakers were also adopted to describe thermodynamic properties related to the hydration of ions [56,54] and/or to the so-called structural entropy, the latter being calculated at the infinite dilution limit [49]. It has also been linked with the dynamic behaviour, both for the viscosity [57] and the diffusion of water in the solutions [58]. Yet another phenomenon has been ascribed to these concepts. Collins and Washabaugh [59], introduced the categories of kosmotrope and chaotrope ions to define the ion-water binding capacity when compared to the attraction experimented by the water molecules to the ionized groups in proteins. They also related the notion of chaotrope to be a protein destabilizer, whilst kosmotropes would stabilize proteins [59,60] and established an analogy between kosmotrope/chaotrope and structure-making/breaking, respectively. However they meant this with regards to the structure of the first solvation shell near an interface, which is very different to the concept previously exposed of structure-maker/breakers within the bulk.

It is also interesting to point out the differences between the shifts in the TMD and the shifts in the freezing temperature of water due to the presence of electrolytes [42]. For a 1 m solution a 1:1 salt provokes a shift of about 4 K in the freezing point of water, and this value does not change significantly for different salts [61]. Thus, up to a concentration of about 1 m of 1:1 electrolyte, the freezing point depression can be considered to be colligative, i.e. a property that does not depend on the nature of the chemical species. However, for a 1:1 electrolyte, even for a concentration as low as 1 m, the shift in the TMD changes for different electrolytes. For instance, from 4 K for LiCl to 19 K for NaI solutions. Thus the TMD is determined fundamentally by structural changes in water due to the addition of the electrolyte, its effects differing considerably upon the nature of the salt. Consequently, variations of the TMD in electrolyte solutions are chemically specific and concentration dependent [28,42]. For not highly concentrated solutions this dependence was empirically established in the Despretz law formulated in the first half of the nineteenth century [33,34]. It states that the TMD shift, defined as

$$\Delta = \text{TMD}_{\text{solution}} - \text{TMD}_{\text{water}}, \quad (1)$$

follows a linear relation with the salt concentration in the molality scale,  $m$  (being the molality the number of moles of solute per kg of solvent):

$$\Delta = K_m \cdot m, \quad (2)$$

where the subindex  $m$  in  $K_m$  indicates that concentrations are given in molality units. Some attempts have been made to solve the puzzle of the shift in the TMD upon the addition of solutes into an expression involving some thermodynamic properties (i.e. partial molar volumes, mixing volumes, entropies, etc). The first one was proposed for non-electrolytes by Wada and Umeda [30], and some others have suggested expressions for electrolytes [37–39,41,62].

For moderate concentrations, the proportionality constant  $K_m$  can be split into group contributions of each of the ions of the electrolyte as follows [42]:

$$K_m = v_+ K_m^+ + v_- K_m^- \quad (3)$$

where  $v_+$  and  $v_-$  stand for the stoichiometry coefficients of the cation and anion, respectively. If this "group contribution" to  $K_m$  is valid within a given concentration regime, an accurate guess for  $\Delta$  might be provided for all combination of salts formed by ions for which values of  $K_m^+$  and  $K_m^-$  are known.

In this work we measured the TMD of several solutions of alkali and alkali-earth metals halides at 1 m concentration. These experiments complete our previous work, in which the TMD of seven salts were measured, namely LiCl, NaCl, KCl,  $\text{MgCl}_2$ ,  $\text{CaCl}_2$ ,  $\text{Li}_2\text{SO}_4$  and  $\text{MgSO}_4$  [42]. Here a set of fourteen new salts are incorporated, namely NaF, KF, CsF, RbCl, CsCl, LiBr, NaBr, KBr, CsBr,  $\text{MgBr}_2$ , LiI, NaI, KI and CsI. This property is also determined by means of Molecular Dynamics simulations with the Madrid-2019 force field (FF) [63,64].

The experimental data of this work will be used as a benchmark for:

- (i) Obtaining group contributions of the shift in the TMD for the ions studied and establishing a Hofmeister-like series for this property based on the individual contributions of the ions.
- (ii) Grasping a rough idea of the effect of individual ions on the local structure of water.
- (iii) Further evaluating the TMD for the Madrid-2019 force field and comparing it with our experimental results.

It should be emphasized in relation with (iii), that evaluating the TMD of electrolyte solutions by means of computer simulation requires a water model able to accurately describe this property. Many popular models (i.e. TIP3P [65], SPC/E [66]) underestimate the temperature of the density maximum by 30–50 K [67], whereas some other models (namely, the TIP4P-Ew [68], TIP4P-D [69] or TIP4P/2005 [70]) are able to reproduce the TMD of pure water. Besides, the TIP4P/2005 yields accurate values for the density of supercooled water [71]. Moreover, it has recently been shown that the Madrid-2019 electrolyte force field [63], which was developed for the TIP4P/2005 water model, describes quite well the TMD at 1 m of 1:1 electrolytes formed by ions of moderate sizes [42]. In 2022 the Madrid-2019 Force Field (FF) was extended to describe larger ions [64]. This FF uses a scaled charge of 0.85 electron units for monovalent ions and 1.7 for divalent ones. The scaling of the charges is based on the electronic continuum approximation, which explicitly accounts for the screening effect of water. It was first proposed by Leontyev and Stuchebrukhov [72–77] and has been further developed by many authors [78–88]. The adequacy of Molecular Dynamics-based results to quantify the experimental data can be discussed in terms of the physicochemical nature of the ionic species at play. We also believe that the prediction of the TMDs should be used in the future to develop and improve current FFs of electrolytes.

## 2. Experimental procedure

In this work we measured the TMD of aqueous solutions of the following salts: NaF, KF, CsF, RbCl, CsCl, LiBr, NaBr, KBr, CsBr,  $\text{MgBr}_2$ , LiI, NaI, KI and CsI. The solutions were made with MilliQ water by weighing the appropriate amount of salt in an AE-240 balance. The purity of all salts was higher than 0.985 in mass fraction. Uncertainty in molality was estimated in  $\pm 0.004 \text{ mol}\cdot\text{kg}^{-1}$ . For measuring the density versus temperature profile, two procedures were used, both based on the determination of the position of the meniscus in capillary glass tubes. The first one is much more precise but uses a quite large volume, around 60 mL. A glass flask with a stopper soldered to a capillary tube is used to this aim. The

flask was submerged in a methanol bath and a temperature sequence was programmed while the meniscus position was recorded using a digital camera. To get the density of the sample as a function of temperature, the density at one reference temperature,  $\rho_0$ , is needed. It has been measured using a DMA 5000 densimeter. The density was thus calculated using:

$$\rho = \rho_0 \frac{V_{f,0} + S_0 L_0}{V_{f,0}(1 + \delta) + S_0 L(1 + 2\delta)(1 + \delta)}, \quad (4)$$

where  $V_{f,0}$ ,  $S_0$  and  $L_0$  stand for the flask volume, the capillary cross section area, and meniscus position at the reference temperature  $T_0$ , respectively.  $L$  is the meniscus position at temperature  $T$ , whereas  $\alpha$  is the glass linear thermal expansivity and  $\delta = \alpha(T - T_0)$ .  $V_{f,0}$ ,  $S_0$  and  $\alpha$  were calculated from calibration experiments with pure water. We observed that this method can be used to measure densities only at temperatures down to around  $-12$  °C. For lower temperatures, the sample cannot be in metastable liquid state and it freezes. It is well known that sample volume is one of key factors for holding the liquid in metastable state. Therefore, we have used the Hare and Sorensen methodology [89], which uses a capillary with very small volume ( $7 \mu\text{L}$ ) for NaI, MgBr<sub>2</sub>, CsI, and NaF, whose temperature of maximum density is expected to be smaller than  $-12$  °C according to MD results. Similarly, the capillary was filled with the sample, sealed and introduced into the methanol bath. A temperature program was applied and the meniscus position was recorded with a digital camera coupled with a stereomicroscope. The density was calculated using Eq. 4, making  $V_{f,0} = 0$ . Uncertainty of both measurement procedures are around  $\pm 5 \cdot 10^{-4} \text{ g}\cdot\text{cm}^{-3}$ , but repeatability of the large volume method is much better, around  $\pm 5 \cdot 10^{-6} \text{ g}\cdot\text{cm}^{-3}$ , than that of Hare and Sorensen, which is roughly two orders of magnitude worse. The density data for each solution were fitted to a third order polynomial form; the TMD was calculated by taking the derivative and equating it to zero. In the case of experiments using the method of Hare and Sorensen we continued the temperature decrease until the capillary broke due to the freezing of the sample. However, in the case of the large volume method, fewer data were collected below the maximum in density. In all cases an expansion of the system was visually observed in the cooling process between the last two measured temperatures (so the TMD must lie between them. See Supplementary Material for a graphical illustration). After the expansion, we only performed one additional measurement in order to elude the crystallization of the sample and the resulting breakage of the apparatus. Therefore, the TMD was not obtained by extrapolation but rather from an interpolation between the temperatures for which we have experimental measurements.

Uncertainty in the TMD was estimated in  $\pm 0.3$  K for the large volume method and in  $\pm 1.5$  K for the capillary method. The density at  $25$  °C was compared with reported data [90,91] for all the studied solutions, with relative deviations below 0.2 per cent for all studied salts. The agreement is quite good considering the claimed uncertainty of these data. More details about the measurement methods can be found elsewhere [89,42]. It should be mentioned that the systems under exploration are metastable with respect to freezing in all cases. In fact the cryoscopic constant of water (which provides the decrease in the freezing temperature of a 1 molal solution) leads to a melting temperature decrease of about 4 or 6 K for a 1:1 or 1:2 electrolyte respectively. These values are smaller than the observed shift in the TMD, as it will be shown later. Thus the TMD is found within the metastable region (with respect to freezing) of the solution. However, since freezing is an activated process, it does not take place instantaneously and it was possible to easily determine the TMD for the 1 m solutions (things of course would be different at higher concentrations, where freezing could certainly occur before reaching the TMD).

Thus we emphasize that in the present experiments of 1 m solutions, no extrapolations were needed to estimate the TMD, since the maxima occurred within the temperature range in which crystallization was still (kinetically) absent. It is interesting to point out that crystallization typically occurred a few degrees below the TMD. This fact might indicate some impact of the TMD on the crystallization kinetics and this problem should be analyzed in more detail in future work.

### 3. Simulation details

Molecular Dynamics simulations were performed in a system comprised by 555 TIP4P/2005 water molecules, 10 cations and 10 anions to achieve 1 m solution. The Madrid-2019 FF [63,64] has been used for the electrolytes. Ion-ion and ion-water parameters were chosen following Ref.[63,64]. We employed the isothermal-isobaric (NpT) ensemble at 1 bar using the GROMACS 4.6.7 package [92]. Temperature and pressure were kept constant by means of the Nosé-Hoover thermostat [93,94] and the isotropic Parrinello-Rahman barostat [95] with a relaxation time of 2 ps, respectively. Simulations run over the temperature range of 250–300 K. The leap frog algorithm [96] with a time step of 2 fs was selected to integrate the equations of motion. A cutoff of  $10 \text{ \AA}$  was set for both the Lennard-Jones (LJ) part of the potential and electrostatic interactions, the latter being treated within the particle mesh Ewald method (PME) [97]. Long range corrections for pressures and internal energies were also included for the Lennard-Jones interaction. Overall, the simulations run between 150–600 ns for each temperature and salt from previously equilibrated configurations. Notice that since the freezing temperature of the TIP4P/2005 model of water is 250 K [98], generally the system in the simulations is not metastable with respect to freezing. However, the temperatures are low and it is necessary to perform longer runs than usual (i.e. simulations should be longer than 50 ns) both to equilibrate the sample and to obtain accurate values of the average density of the system. As an example, we present the behavior of the density (a) and potential energy (b) of a 1 m LiBr aqueous solution at 260 K in Fig. 1. As can be seen the system is well equilibrated and there is no drift of either the density or the potential energy of the system. All simulations performed in this work span around  $25 \mu\text{s}$ . The temperature-density profile is finally fitted to a third order polynomial from which the TMD is analytically located. The estimated error in the TMD obtained from simulation is  $\pm 2$  K. In the Madrid-2019 model the value of the charge of the ions is constant regardless of the density of the system. Recently, Kolafa [99] has suggested that when considering electrolyte solutions in a wide range of densities, the value of the scaled charge should be modified accordingly. This interesting idea could be considered in future work. However, notice that for each salt the density varies very little in the temperature range around the TMD and therefore, keeping the value of the scaled charge constant in this work seems to be a reasonable approach.

### 4. Results

In Fig. 2 we present the experimental and simulation results for the density-temperature profiles. The data are grouped according to the halide anion, independently on the cation. A summary of the TMD and the densities at the TMD can be found in Table 1. It must be noticed that the TMD for some of these solutions were previously determined [28], but only up to molalities much lower than  $1 \text{ mol}\cdot\text{kg}^{-1}$ , a fact that makes an eventual comparison not feasible. However, for NaCl and LiCl we found previously reported experimental values [28] at 1 m and they were compared to our experimental results in our previous work [42], finding excellent

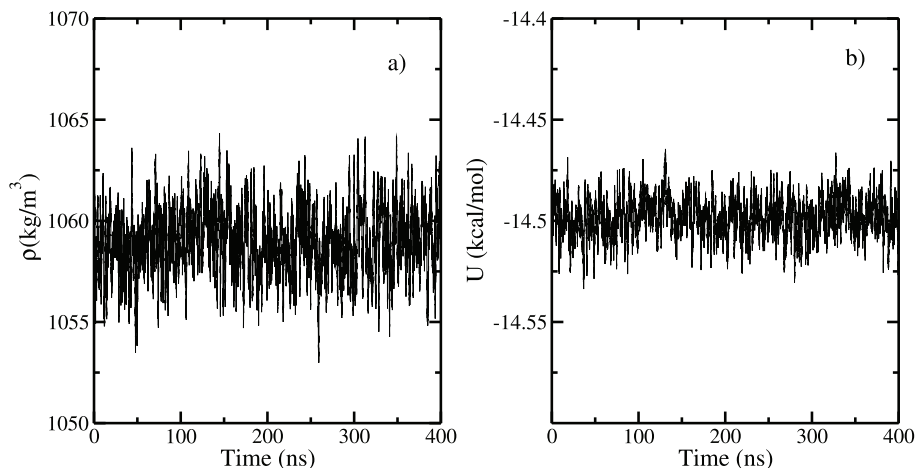


**Fig. 1.** Equilibrated system along the simulation time. (a) Density and (b) Potential energy per particle for a system containing 555 water and 20 ions of a LiBr aqueous solution 1 m at 260 K. To facilitate the visual presentation we have displayed the rolling averages of both density and potential energy.

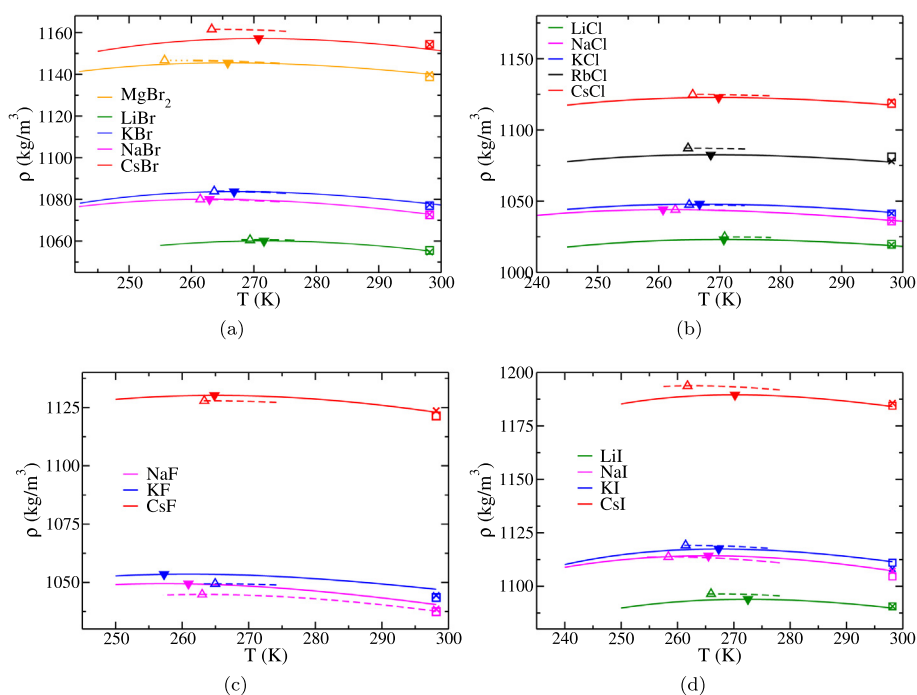


**Fig. 2.** Density for various halide solutions at 1 m as a function of the temperature at room pressure. Solid lines: simulations for the Madrid-2019 model. Dashed lines: experiment. Dotted lines: extrapolation from experimental results. TMD: empty up triangles (experiment), filled down triangles (simulations). Density at room temperature from experiments: crosses (results from Ref.[90] and Ref.[28]); empty squares (results from this work). The data for LiCl, NaCl and KCl were obtained from our previous work [42].

agreement. Simulations are able to describe fairly well the temperature dependence of the density of the solutions down to the density maximum. Deviations between the experimental and the calculated densities at their maxima are always smaller than 0.5%. Thus the FF is very accurate for density predictions even for the rather large ions considered in this work ( $I^-$ ,  $Rb^+$  and  $Cs^+$ ). For fluoride solutions, the sign of the deviations indicates that the Madrid-2019 FF slightly overestimates the experimental values. An interesting observation is that the (mass) densities of sodium and potassium solutions are quite similar for all the halide series. That was already true at room temperature and the results of this work show that this similarity in density between NaCl and KCl is also present in the supercooled regime down to 260 K. It is worth mentioning that there is a small offset between the experi-

mental and simulation densities along the studied temperature range, implying that the equation of state does not deteriorate considerably at lower temperatures. For the rest of the halides the predictions of the densities from simulations are in excellent agreement with those from experiments. In Fig. 2(a) simulation and experiments are also displayed for a solution containing magnesium. It can be seen that the density prediction as a function of temperature is also quite good for divalent cations (see also Table 1).

As for the predictions for the temperature at which the maximum in density occurs, the deviations found in this property are bigger than those just discussed here for the density and than the deviations of the TMDs reported in our previous work for chloride and sulfate solutions with the Madrid-2019 model [63], which

**Table 1**

Temperature of maximum density and the density at the TMD of the electrolyte solutions at a concentration of 1 m. Dev. and Dev. (%) stand for deviations of the simulated from experimental results and the deviation percentage, respectively. Salts starting from LiCl are the results of our previous work [42]. Salts for which the deviation between simulation and experiment for the TMDs is larger than 5 K are marked in bold.

Salt	TMD (K)				Maximum in density (kg·m <sup>-3</sup> )			
	Exp.	Madrid-2019	Dev.	Dev. (%)	Exp.	Madrid-2019	Dev.	Dev. (%)
NaF	263.2	257.3	<b>5.9</b>	2.2	1044.8	1049.5	-4.7	-0.4
KF	265.0	260.9	4.1	1.5	1049.4	1053.2	-4.1	0.4
CsF	263.3	264.8	-1.5	-0.6	1127.9	1129.9	-2.0	-0.2
RbCl	264.8	268.5	-3.7	-1.4	1087.2	1082.3	4.9	0.5
CsCl	265.6	269.8	-4.2	-1.6	1125.0	1123.0	2.0	0.2
LiBr	269.4	271.6	-2.2	-0.8	1060.4	1059.8	0.6	0.1
NaBr	261.4	263.2	-1.5	0.6	1080.0	1079.8	0.2	0.0
KBr	263.6	266.8	-3.2	-1.2	1083.6	1083.5	0.1	0.0
CsBr	263.2	270.8	<b>-7.6</b>	-0.9	1161.6	1157.1	4.5	0.4
MgBr <sub>2</sub>	258.1	263.9	<b>-5.8</b>	-2.2	1146.9	1145.4	1.5	0.1
LiI	266.0	272.5	<b>-6.5</b>	-2.4	1096.4	1094.1	2.3	0.2
NaI	258.3	265.5	<b>-7.2</b>	-2.8	1113.8	1114.6	-0.8	-0.1
KI	261.4	267.3	<b>-5.9</b>	-2.3	1119.0	1117.3	1.7	0.2
CsI	262.8	270.2	<b>-7.4</b>	-2.8	1193.8	1189.7	4.1	0.3
LiCl	270.8	270.7	0.1	0.0	1024.8	1023.1	1.7	0.2
NaCl	262.7	260.7	2.0	0.8	1044.0	1044.0	0.0	0.0
KCl	265.0	266.7	-1.7	-0.6	1047.5	1047.9	-0.4	-0.0
MgCl <sub>2</sub>	261.3	265.5	-4.2	-1.6	1076.5	1073.5	3.0	0.3
CaCl <sub>2</sub>	253.6	252.4	1.2	0.5	1092.4	1092.2	0.2	0.0
Li <sub>2</sub> SO <sub>4</sub>	256.1	254.9	1.4	0.55	1091.4	1089.3	2.1	0.2
MgSO <sub>4</sub>	253.9	257.8	-3.9	-1.5	1118.9	1115.8	-3.1	-0.3

are also included in Table 1 for comparative purposes. Taking into account that the uncertainty in the estimates from simulations is of about 2 K, and that from experiments is around 1.5 K, a deviation of the TMD larger than 4 K is out of the combined uncertainty range and can be regarded as some deficiency in the FF. For some of the salts measured in this work the deviation is much larger than 4 K. In Table 1 salts for which the deviation between simulation and experiment for the TMDs is larger than 5 K are marked in bold. Particularly, for the fluoride solutions, the simulations yield lower TMDs than the experimental ones except for the CsF. This anomaly can be explained by a cancellation of errors, since the Madrid-2019 model of Cs<sup>+</sup> tends to overestimate the TMD. Regarding the bromide solutions, the TMDs predicted by simulation are slightly higher than the experimental ones, although the estimates for LiBr, NaBr and KBr solutions are quite accurate. Finally, the values for the TMDs of the iodide solutions studied by simulation are even further away from the experimental ones, laying the density maxima always at higher temperatures for the Madrid-2019 FF. One fact that could be detrimental for the estimation of the maximum in density of the iodide solutions by the Madrid-2019 model is that the obtained I<sup>-</sup>-oxygen distance is considerably below (3.28 Å) than the experimental ones (~ 3.6 Å) [100–102].

In view of these results, what can be laid out is that in simulations using the Madrid-2019 FF, fluorides underestimate the TMD values, chlorides perform rather well when predicting this property and, as the size of the anion increases (bromide and iodide) there is a systematic overestimation of the TMD of the solutions. Iodide is a large anion and a very polarizable one, so its macroscopic behaviour is determined largely by the deformation of the electronic structure when interacting with other atoms and/or molecules, i.e. polarization will be playing an important role in these large ions. Kalcher et al. claimed that many-body effects were significant at concentrations above 0.5 M for KF and NaI solutions [103]. It is thus conceivable that electrolyte FFs including many-body effects could outperform pair potential-based FFs regarding the estimation of the TMD [104–107]. In the case of fluoride, it should be mentioned that the anion can break the molecule of water *via* hydrolysis (with a non-negligible hydrolysis constant of 6.8·10<sup>-4</sup>) and this chemical process can not be accounted by the FF considered in this work. We hope that our

experimental results will be used in the future to further develop FFs for ions in water as well as to test electrolyte FFs [108,109,104,110,82,111,106,112,113] for its capacity to predict the TMD of aqueous solutions.

A closer inspection of these curves allows us to compare the curvature of the temperature-density profile of the different salts in solution. To that aim we locate the origin of coordinates at the experimental values of the TMD and the maximum in density. Results are shown in Fig. 3(a) for Li<sup>+</sup> salts and in Fig. 3(b) for Na<sup>+</sup> salts. Results for water are also shown for reference. The presence of salts flatten the curvature with respect to that of pure water except for the striking case of NaI, in which the curvature is almost identical to that of pure water. It is also interesting to notice that for the lithium halides, the curvature is very similar regardless of the anion, whereas the opposite is observed for Na<sup>+</sup> halides, where no correlation can be established between the curvature and the anion size.

Let us now discuss the impact of the different ions in the total volume of a 1 m aqueous solution. By representing the volume instead of the density, the effects of mass dependencies can be avoided. Although the volumes were obtained from experiments, we present the value that a sample having 555 molecules of water would occupy. Certainly, one could present the volume of a system containing 1 kg of water, but we found it convenient to present it in this way to be consistent with our previous work [42]. Basically, we converted the volume occupied by a 1 m solution with 1 kg of water to the volume that it would occupy when containing only 555 molecules of water. Nevertheless, the discussion will be restricted to 1:1 salts to avoid misunderstandings originated by stoichiometric effects, i.e., we dismiss Mg<sup>2+</sup>, Ca<sup>2+</sup> and SO<sub>4</sub><sup>2-</sup> from the analysis. In Fig. 4 we present the ion-dependent trends in the volume-temperature profile. For salts with a common anion, the volume of the solutions increases with the volume of the cation except for lithium solutions. Despite being the smallest cation in the alkali series, lithium solutions are not those with the smallest volume, but rather they have larger volumes than Na<sup>+</sup> solutions in all cases (i.e., chlorides, bromides and iodides). Thus Li<sup>+</sup> provokes an anomalous expansion of the volume of the system. This was discussed in our previous work [42] for the case of LiCl, where, as suggested by a structural study carried out by Nguyen et al. [20], the

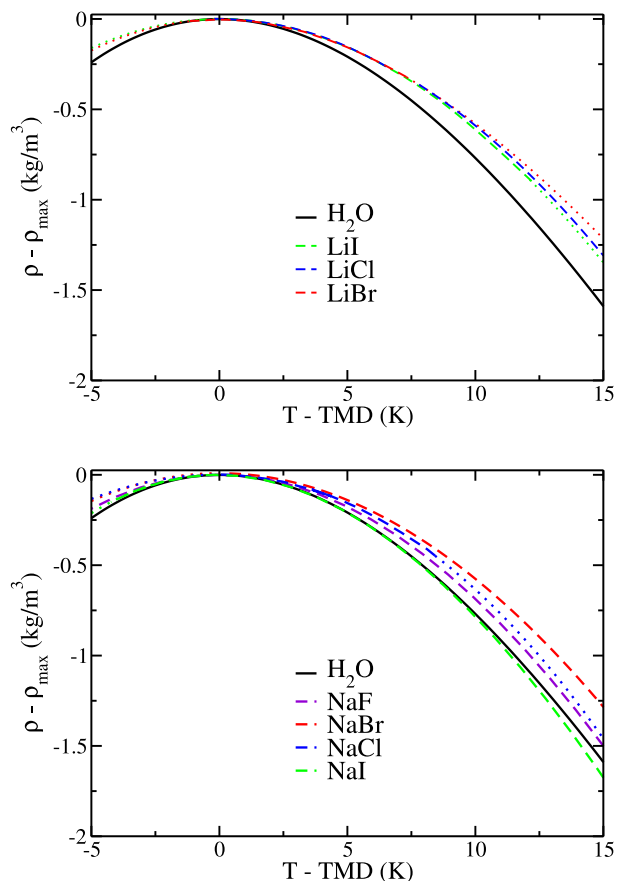


**Fig. 3.** Scaled densities at 1 m solutions for salts containing (a)  $\text{Li}^+$  or (b)  $\text{Na}^+$ . Pure water taken from Ref. [114]. The values for LiCl were obtained from our previous work [42].

high electronic density of  $\text{Li}^+$  would create the presence of voids within the first solvation shell and between the first and the second one, also leading to a rotational hindering of the water molecules coordinated to this ion, thus resulting in an expanded configuration of water in lithium chloride solutions. Assuming this can be generalized for the rest of the  $\text{Li}^+$  solutions, it would be a possible explanation for the observed anomaly. It is also interesting to notice the temperature dependence of the volume of lithium solutions is slightly different to that of the rest of the salts. Whereas for most of the salts, the density curves are almost parallel to each other, this is not the case for salts containing  $\text{Li}^+$ . Interestingly at 278 K the volumes of NaI and LiI are identical. At this point the smaller size of  $\text{Li}^+$  with respect to  $\text{Na}^+$  is compensated exactly by the ordering provoked in the molecules of water. It is also striking the small difference in volume between the bromide and chloride solutions. Although  $\text{Br}^-$  is larger than  $\text{Cl}^-$ , the volume of solutions containing these two anions are similar (when compared to the same cation). These results are in agreement with the conclusions reached by Nilsson et al. for alkali halide solutions employing X-ray spectroscopy in which they observed structural similarities between  $\text{Br}^-$  and  $\text{Cl}^-$  regardless of the cation, whereas iodide solutions undergo significant H-bonds disruption [50].

In an attempt to understand what happens with the volume occupied by water in the solutions, we shall compute the so called "free volume" ( $V_{free}$ ), which is obtained by subtracting the volume occupied by the ions to the total volume of the solution by using the following expression:

$$V_{free} = V - \frac{4}{3} \pi \sum_{\pm} N_{\pm} (d_{\pm-O_w} - r_{w-\pm})^3, \quad (5)$$

where the sum runs over all type of ions (i.e.  $\pm$ ),  $N_{\pm}$  represents the number of ions of a certain species and  $d_{\pm-O_w}$  is the distance between the oxygen atom of water and the cation (+) or anion (-) as obtained from experimental diffraction studies. Due to experimental discrepancies regarding the distance between ions and the

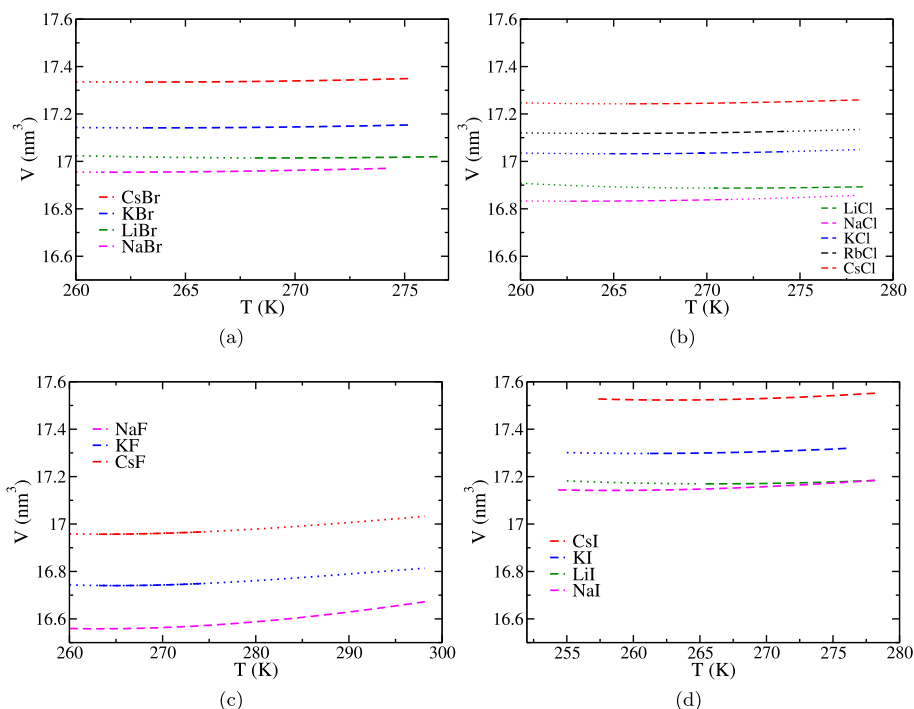


**Fig. 4.** Volume computed from experimental densities for various halide solutions at 1 m and 1 bar as a function of temperature. Dashed lines: experiment. Dotted lines: extrapolation of experimental data obtained from cubic polynomial fits. The volume presented is obtained from experiments, but represents that of a 1 m solution having 555 molecules of water. See text for details. Required information of LiCl, NaCl and KCl salt were obtained from our previous work [42].

oxygen of water, we have taken the mean value provided by Marcus in his review [19]. The term  $r_{w-\pm}$  is the distance that ought to be subtracted from the water-ion distance to estimate the radius of the ion in solution (i.e., it represents the radius of a water molecule). This is quite a delicate step when calculating the free volume. Marcus estimated the radius of the molecule of water to be 0.138 nm and uses this value both for the cations and for the anions in Eq. 5. However, Schmid et al. proposed two different radii for water molecules depending on whether they solvate a cation or an anion [115]. In particular, Schmid et al. suggested to use 0.063 nm and 0.140 nm for cations and anions, respectively. There is a reasonable physical picture underlying this approach, since the hydrogen atoms of water are pointing towards the anion in the first coordination shell, whereas for cations, the closest atom from the neighbouring water molecules is an oxygen. In Fig. 5 the free volume of alkali iodide solutions is plotted as evaluated from both Marcus' and Schmid's approaches. It is apparent that depending on the radius assigned to water in contact with ions, the conclusions that can be drawn are conflicting, being the free volumes thus obtained completely different. Besides, the considerable uncertainty regarding the experimental value of  $d_{\pm-o_w}$  for many electrolytes [19,52], also makes it difficult to establish definitive conclusions.

Even admitting to the arbitrariness when computing free volumes, the more physical-like approach of Schmid would explain the anomalous volumes of  $\text{Li}^+$  solutions. It is worth mentioning that the Schmid radii were quite useful for estimating the hydration free energies of a number of ions [116] and for correcting the hydration energy of electrolyte FFs using scaled charges [117]. The question as to whether the shift in the TMD can be correlated to the free volumes may arise if the lowering of the maximum in density is understood as a stabilization of the HDL over the LDL (that is, the high density liquid could exist at lower temperatures upon the addition of salt). This so-called "temperature-like effect" of ions has been suggested previously by Nilsson and coworkers [50,118]. Therefore, the assumption would be that large free volumes correspond to small shifts in the TMD while small free volumes would imply a bigger impact on the TMD. This might justify the behavior found for lithium, potassium and cesium salts, but sodium salts can not be rationalized this way. However, the free volume using Schmid approach does indeed follow the same order as the viscosity of water in the solutions, that is,  $\text{Li}^+ > \text{Na}^+ > \text{K}^+ \approx \text{Cs}^+$  [119,120].

Since salts dissociate into ions when dissolved in water and considering that 1 m solutions have approximately 28 molecules of water per ion (i.e. two coordination layers), it seems reasonable to neglect ion-ion interactions due to the screening of water, in

which case  $\Delta$  could be described by using a group contribution method. In this framework, the experimental value of the shift in the TMD can be obtained as a contribution from the cation and another one from the anion under the supposition that these are additive. In our previous work, we provided the individual ion contributions  $K_m^\pm$  for several ions (i.e.,  $\text{Li}^+$ ,  $\text{Na}^+$ ,  $\text{K}^+$ ,  $\text{Ca}^{2+}$ ,  $\text{Mg}^{2+}$ ,  $\text{Cl}^-$ ,  $\text{SO}_4^{2-}$ ) [42]. Following the same approach, we have computed the ion contributions for the rest of the halides ( $\text{F}^-$ ,  $\text{Br}^-$ ,  $\text{I}^-$ ) and for big alkali metal cations ( $\text{Cs}^+$  and  $\text{Rb}^+$ ). To that aim, we have proceeded as follows: from the experimental value of  $\Delta$  for 1 m solutions we evaluated  $K_m$  from Eq. 2. Applying Eq. 3 with the appropriate stoichiometric coefficients and the previously reported values of  $K_m^\pm$  [42], the unknown contributions are easily evaluated for each salt. The values of  $K_m^\pm$  for each ion are averaged and the final results are summarized in Table 2. Notice that values of  $K_m^\pm$  are relative and were initially determined arbitrarily by taking the shift of LiCl as a reference and assigning half  $\Delta$  to each ion [42], whereas  $K_m$  is an absolute value determined by the shift in the TMD upon the addition of some amount of salt. In short, the  $K_m$  of a certain salt does not depend on any arbitrary selection. However the individual values for ions of  $K_m^\pm$  depend on the choice made for a reference ion (in our case  $\text{Li}^+$ , for which we assigned a  $K_m^\pm$  value of  $-3$ ). It should be stressed though, that when considering a series of salts with a common ion (i.e., LiCl, NaCl, KCl, RbCl, CsCl) the differences in  $K_m$  for the salts are just the differences of  $K_m^\pm$  of the cations and therefore these differences do not depend on any arbitrary choice.

A comparison between the values of  $\Delta$  determined experimentally and those obtained from the group contribution approach is shown in Table 3. By using these individual  $K_m^\pm$  coefficients of Table 2 it is possible to reproduce the shift in the TMD with a deviation from the experimental value smaller than 1 K for most of the cases. The results of Table 3 show that cation-anion interactions contribute very little to the shift in TMD when the concentration is 1 m. Otherwise, one could not predict so accurately the TMD using the group contribution approach. Of course, at much higher concentrations, cation-anion interactions would also impact the value of the shift in the TMD. The predicted values of the remaining salts comprised by the ions presented in Table 2 are collected in the bottom part of Table 3.

Finally, a couple of comments on the experimental and computational solubilities should be specified. First, in Table 3 we have included the experimental solubilities of each salt at 25 °C. A decrease in the temperature to 0 °C leads to a solubility decrease of, at most, 20–30 % for these salts, but since most of them have high solubilities, this does not pose a threat of approaching the solubility limit at the lowest temperatures considered in this work,

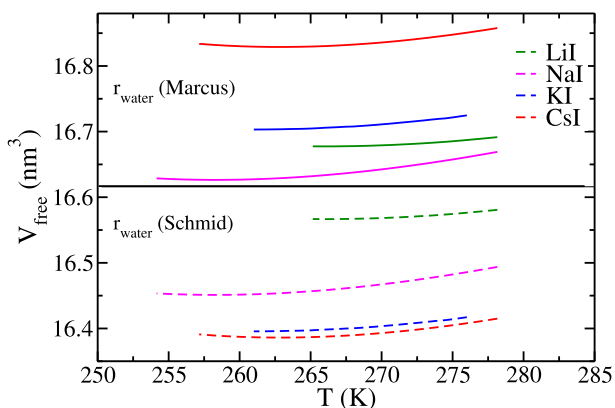


Fig. 5. Free volume for 1 m iodide solutions at 1 bar as a function of temperature obtained from Eq. 5. Solid lines: using Marcus' radius for water in solution (top). Dashed lines: using Schmid's radius for water in solution (bottom).

Table 2

Individual Despretz coefficients,  $K_m^\pm$ , for the ions considered in this work as obtained from the experimental TMD values. The coefficients were obtained from the combination of the experimental  $\Delta$  data and the  $K_m^\pm$  values obtained previously in Ref.[42], also shown here (bottom part).

Ion	$K_m^\pm$ (K·kg·mol <sup>-1</sup> )
Rb <sup>+</sup>	-5.4
Cs <sup>+</sup>	-8.4
F <sup>-</sup>	-3.7
Br <sup>-</sup>	-4.8
I <sup>-</sup>	-7.1
Li <sup>+</sup>	-3.0
Na <sup>+</sup>	-11.6
K <sup>+</sup>	-8.8
Mg <sup>2+</sup>	-8.3
Ca <sup>2+</sup>	-17.6
Cl <sup>-</sup>	-3.2
SO <sub>4</sub> <sup>2-</sup>	-15.8

**Table 3**

Shift in the TMD of different salt solutions at a 1 m concentration measured experimentally and calculated from the individual group contribution approach. Results from our previous work are also reported (between LiCl and MgSO<sub>4</sub>) [42]. In the bottom part (starting from LiF) we present the predictions of the TMD shift as obtained from Despretz law for salts that have not been measured experimentally yet. We believe these predictions are probably accurate given the excellent agreement shown in the upper part of the Table for salts where the experimental TMD is known. Experimental solubilities for each salt at 25 °C (in mol·kg<sup>-1</sup>) are taken from Ref. [122].

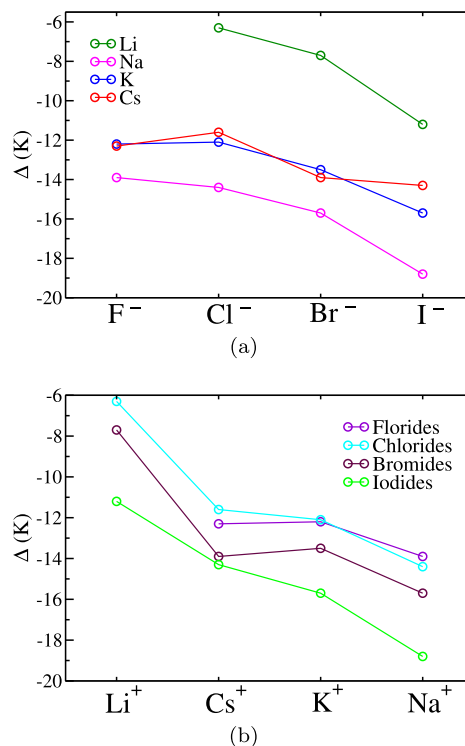
Salt	$\Delta_{Exptl}$ (K)	$\Delta_{Group}$ (K)	Solubility at 25 °C (m)
NaF	-13.9	-15.3	0.99
KF	-12.2	-13.1	17.50
CsF	-12.3	-12.1	37.70
RbCl	-12.3	-12.3	7.77
CsCl	-11.6	-11.6	11.30
LiBr	-7.7	-7.8	20.84
NaBr	-15.7	-16.4	9.20
KBr	-13.5	-13.6	5.77
CsBr	-13.9	-13.6	5.77
MgBr <sub>2</sub>	-19.1	-17.9	5.60
LiI	-11.2	-10.1	12.33
NaI	-18.8	-18.7	12.40
KI	-15.7	-15.9	8.92
CsI	-14.3	-15.4	3.26
LiCl	-6.2	-6.2	19.95
NaCl	-14.3	-14.8	6.15
KCl	-12.0	-12.0	4.81
MgCl <sub>2</sub>	-15.7	-14.7	5.81
CaCl <sub>2</sub>	-24.0	-24.0	7.30
Li <sub>2</sub> SO <sub>4</sub>	-20.9	-21.8	3.12
MgSO <sub>4</sub>	-23.1	-24.1	3.07

Salt	$\Delta_{Exptl}$ (K)	$\Delta_{pred,1m}$ (K)	Solubility at 25 °C (m)
LiF	-	-6.7	0.05
CaF <sub>2</sub>	-	-25.0	0.0002
MgF <sub>2</sub>	-	-15.7	0.002
RbBr	-	-10.2	7.01
CaBr <sub>2</sub>	-	-27.2	7.65
RbI <sub>2</sub>	-	-19.6	7.76
CaI <sub>2</sub>	-	-31.8	7.30
MgI <sub>2</sub>	-	-22.5	5.20
Na <sub>2</sub> SO <sub>4</sub>	-	-39.0	1.96
K <sub>2</sub> SO <sub>4</sub>	-	-33.4	0.69
Rb <sub>2</sub> SO <sub>4</sub>	-	-26.6	1.90
Cs <sub>2</sub> SO <sub>4</sub>	-	-32.6	5.03
CaSO <sub>4</sub>	-	-33.4	0.02

except for maybe the case of the NaF solution. It must be noticed that, although this salt is not soluble up to 1 m, we managed to achieve homogeneity by heating the sample. No precipitation of the salt was observed when cooling the sample in the experiments. The system is again in a metastable state (in this case in a doubly metastable state as the system is both metastable with respect to freezing of ice and precipitation of the salt). Secondly, it ought to be mentioned that, although the solubilities of the Madrid-2019 force field are unknown, the number of contact ion pairs (CIP) at the solubility limit of each salt are low by design of the force field [64,121].

Certain regularities can be established for the shift in the TMD that can be useful to understand the impact of each ion individually. In Fig. 6 we show the shift of different salts having a common cation as a function of the anion (a) or having a common anion as a function of the cation (b). In absolute values, for salts with a common cation, the shift in the TMD remains approximately constant from F<sup>-</sup> to Cl<sup>-</sup>, increases from Cl<sup>-</sup> to Br<sup>-</sup>, and from Br<sup>-</sup> to I<sup>-</sup>. This is true for all the series of cations. Therefore, larger anions provoke larger shifts in the TMD. To some degree, the impact of anions on the TMD is regular and simple: it follows the size of the anion (except for F<sup>-</sup> and Cl<sup>-</sup> which have similar shifts). Besides, the fact that the trends for different cations are almost parallel indicates that the contribution of each anion to the TMD is constant and does not depend on the counterion. The only exception is CsI, which



**Fig. 6.** Experimental results of the shift in the TMD for 1 m solutions as a function of the anion (a) and of the cation (b). Required information of LiCl, NaCl and KCl salt were obtained from our previous work [42].

seems not to follow this rule. It has been suggested that ions with similar sizes might be prone to forming CIPs [123,124]. Moreover CsI has a significant number of CIP even at low concentrations [101] which might be the reason for the slightly different behavior of CsI shown in Fig. 6(a). An interesting observation is that the curves of K<sup>+</sup> and Cs<sup>+</sup> in Fig. 6(a) are practically identical. Thus, K<sup>+</sup> and Cs<sup>+</sup> provoke almost identical shifts in the TMD.

Regarding the order in  $\Delta$  for the cations (Fig. 6(b)), Li<sup>+</sup> induces the smallest shift in the TMDs followed by K<sup>+</sup> and Cs<sup>+</sup>, being Na<sup>+</sup> the monovalent cation with the biggest  $\Delta$  for all the halide salts. Therefore, a size correlation can not be established. This asymmetry in the behavior of cations and anions, points out the dramatic differences in their hydration.

Whether the anions or the cations are responsible for more significant changes upon the structure of water has been widely debated in the literature due to conflicting results among different spectroscopy techniques [50,118,125,126]. In this work, we conclude from straightforward experimental measurements that cations induce more complex changes upon the structure of water than anions as far as the TMD is concerned.

Finally, we propose a classification for the ions based on the impact they have on the TMD. In Fig. 7 this is shown for the cations (a) and for the anions (b). The TMD can be measured experimentally and the results of Fig. 6 show clear trends that do not require any interpretation nor do they entail ambiguity. Besides, this ordering is also found by other authors concerning the TMD [38] and the effect of ions on the structure of water [127]. The Hofmeister series has become a recurring attempt to unify the effect of ionic species, both on the bulk properties of aqueous solutions and on protein-related events. Historically, Hofmeister classified ions by their capacity to precipitate proteins in a solution [128], which shows how the chemical potential of proteins changes in the presence of ions, as proteins precipitate when their chemical potential in solution matches that of the protein in the solid phase.

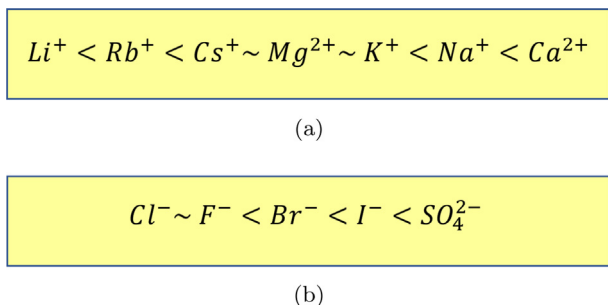


**Fig. 7.** Order of the shift (in absolute value) in the TMD for the ions studied in this work. (a) Cations; (b) anions. Ions on the left provoke small shifts in the TMD with respect to pure water, and ions on the right provoke a large shift in the TMD with respect to pure water.

Later, these qualitative ordering was generalized to other biological-related properties [129]. However, due to the very unclear terms used throughout the literature of ‘structure-making/breaking’ alluding to the structure of bulk water in electrolyte solutions, these were mixed with those used to describe the Hofmeister series [49] (this is discussed in Section I). More recently, many other authors have rightfully claimed that this dogma of arranging ion-specific behaviour in water into a simple qualitative order is wrong, since it has been proved that the main contributions to the Hofmeister effect are the surface and electrostatic water-protein interactions rather than bulk water effects [130,49,59,131]. Following the later approach, our series does not state anything about the ordering of water, it just reflects the impact of each ion on the TMD. Obviously a ‘Hofmeister-like’ series can be developed for each experimental property.

It is tentative to think that ions with a large shift in the TMD do so because they break the structure of water to a larger extent than ions with comparatively smaller shifts in the TMD. This would mean that  $Li^+$  and  $F^-$  would be structure makers and  $Na^+$  and  $I^-$  would be structure breakers, being  $Cs^+$ ,  $K^+$ ,  $Cl^-$  and  $Br^-$  in between. However it seems naïve to believe that there is an universal Hofmeister series that explains all the properties of electrolytes in water, since each ion affects each property in a different way. A simple example would be the viscosity ( $\eta$ ) of alkali chloride salts in solution [132]. In Fig. 8 the experimental  $\Delta$  and the values of the viscosity for alkali chloride solutions are presented. As can be seen, the solution with the largest viscosity is that of LiCl, being the viscosities of CsCl, KCl and RbCl solutions quite similar and significantly smaller than that of LiCl. However, the viscosity of the NaCl solution is higher than that of CsCl, KCl and RbCl, although slightly smaller than that of LiCl, whereas in the TMD series LiCl has the smallest shift and NaCl the largest one so that they are at the extremes of the series.

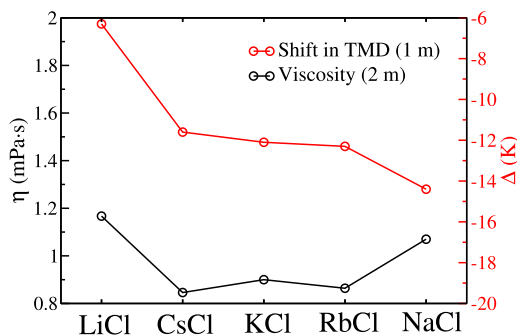


**Fig. 8.** Left axis: viscosities of 2 m solutions of alkali metal chlorides from Refs. [120,119]. Right axis: shift in the TMD ( $\Delta$ ) of 1 m solutions of alkali metal chlorides.

It can be easily deduced that in the ‘Hofmeister-like’ series for viscosities,  $Na^+$  is between  $Li^+$  and ( $K^+/Cs^+/Rb^+$ ), whereas in the ‘Hofmeister’ series for TMD it is at the other extreme from  $Li^+$ .  $Na^+$  occupies two different positions in the Hofmeister series of both properties. This is a clear example that there is no universal ‘Hofmeister’ series explaining all properties. Besides, in our opinion, describing these Hofmeister series in terms of the ‘ordering’ of water is dangerous and leads to inconsistencies. Bearing in mind that with ‘ordering’ we mean ‘strengthening of the H-bond network’, if the rule of thumb is ‘larger ordering of water, larger viscosity’ and ‘small shift in the TMD’, one arrives to a conflict with  $Na^+$ , since it would ‘order’ water according to the viscosity criteria while disordering it according to the TMD series. Hence, in the case of the cation  $Na^+$  shown in Fig. 8, there are other processes in addition to H-bond disruption that must affect the considered properties. In conclusion, from our point of view, one should not use the terms ‘ordered water’ or ‘disordered water’ since they are ambiguous, but simply realize that the impact of each ion on a certain property follows an observable trend.

## 5. Conclusions

In this work we have determined experimentally the TMD of 1 m aqueous solutions of fourteen different salts. In a previous work [42], we measured this maximum for a set of seven different but complementary salts. Overall the experimental values of the TMD for twenty-one common salts comprising alkaline and alkaline-earth halides, chlorides, and some sulfates, are now available. These results are quite useful to understand the impact of different ions upon the structure of water and should be used as a target property in the design of new FFs for electrolytes.

Here we have shown that the Madrid-2019 FF [63,64] (which combines the TIP4P/2005 [70] model of water and scaled charges for the ions) predicts extraordinarily well the densities for a wide range of temperatures and the density at the maximum itself. With respect to the computational predictions of the TMD, their deviations from the experimental data are less than 4 K (which is within the combined uncertainty of simulations and experiments) for most of the salts. However, when large ions are involved ( $Cs^+$ ,  $Rb^+$  and  $I^-$ ), the model is not so successful in reproducing the TMD. Further work is needed to understand the origin of the deviation but most likely the lack of polarizability of the FF is responsible for that.

By collecting all the experimental values, we were able to establish the contribution of each ion to the TMD following a group contribution approach. It turns out that the magnitude of the shift (i.e. the absolute value of  $K_m^\pm$ ) increases with the size of the anion (i.e.  $F^- < Cl^- < Br^- < I^- < SO_4^{2-}$ ). However in the case of cations, the size of the cation is not enough to describe the experimental shifts. They follow the ordering  $Li^+ < Rb^+ < K^+ \simeq Cs^+ < Na^+ < Ca^{2+}$ . In fact, for monovalent ions  $Na^+$  is the most efficient cation in shifting the TMD down, despite its relatively small size. In the case of divalent ions,  $Ca^{2+}$  is the most efficient in shifting the TMD. According to these observations, a ‘Hofmeister-like’ series is established to identify the capacity of each ion for shifting the maximum in density to lower temperatures with respect to pure water.

A final word of caution: the ordering of the ions found in this work for the shift in the TMD should not be used to order other properties. Actually, for viscosities the ordering of the monovalent cations is  $Li^+ > Na^+ > Cs^+ \simeq K^+ \simeq Rb^+$ . As can be seen, the position of  $Na^+$  is changed in the TMD-based and in the viscosity-based series, indicating that each ion affects different properties in a different way. In our opinion, an universal Hofmeister series explaining the ordering of all dynamic and static properties of electrolytic solutions can not be established. However, in the case of the

TMD, the ordering is straightforward, but further work is needed to unravel the molecular origin of the sequence found in the experiments. The TMD is a relatively simple property and certainly its value is related to the changes provoked by ions upon the structure of water. We have found the cations to have a more complex and overall extensive impact upon the structure of water than anions (at least for the halides series) in terms of the TMD. To understand the impact of ions on water at a molecular level, it is absolutely needed to provide insights into how ions modify the TMD of pure water, because it is a true fingerprint that reflects the structure and tetrahedral ordering of water. This task is on the table for the entire community now.

### Data availability

Data will be made available on request.

### Declaration of Competing Interest

The authors declare that they have no known competing financial interests or personal relationships that could have appeared to influence the work reported in this paper.

### Acknowledgment

This project has been funded by grants PID2019-105898 GB-C21 and PID2020-115722 GB-C22 of the Ministry of Science, Innovation and Universities.

### Appendix A. Supplementary material

Supplementary data associated with this article can be found, in the online version, at <https://doi.org/10.1016/j.molliq.2023.121433>.

### References

- [1] D. Eisenberg, W. Kauzmann, *The Structure and Properties of Water*, Clarendon, Oxford, 1969.
- [2] P.H. Poole, F. Sciortino, U. Essmann, H.E. Stanley, Phase behavior of metastable water, *Nature* 360 (1992) 324–328.
- [3] G. Pallares, M.E.M. Azouzi, M.A. González, J.L. Aragonés, J.L.F. Abascal, C. Valeriani, F. Caupin, Anomalies in bulk supercooled water at negative pressure, *Proc. Nat. Acad. Sci.* 111 (2014) 7936–7941.
- [4] T.E. Gartner, L. Zhang, P.M. Piaggi, R. Car, A.Z. Panagiotopoulos, P.G. Debenedetti, Signatures of a liquid–liquid transition in an ab initio deep neural network model for water, *Proc. Nat. Acad. Sci.* 117 (42) (2020) 26040–26046.
- [5] L. Xu, P. Kumar, S.V. Buldyrev, S.H. Chen, P.H. Poole, F.S.H.E. Stanley, Relation between the widom line and the dynamic crossover in systems with a liquid–liquid phase transition, *Proc. Natl. Acad. Sci. U.S.A.* 102 (2005) 16558–16562.
- [6] A. Nilsson, L.G.M. Pettersson, The structural origin of anomalous properties of liquid water, *Nat. Commun.* 6 (2015) 8998.
- [7] R.J. Speedy, C.A. Angell, Isothermal compressibility of supercooled water and evidence for a thermodynamic singularity at  $-45$  degrees c, *J. Chem. Phys.* 65 (1976) 851–858.
- [8] H. Tanaka, Bond orientational order in liquids: towards a unified description of water-like anomalies, liquid–liquid transition, glass transition and crystallization, *Eur. Phys. J. E: Soft Matter Biol. Phys.* 35 (2012) 113.
- [9] P. Gallo, K. Amann-Winkel, C.A. Angell, M.A. Anisimov, F. Caupin, C. Chakravarty, E. Lascaris, T. Loerting, A.Z. Panagiotopoulos, J. Russo, J.A. Sellberg, H.E. Stanley, H. Tanaka, C. Vega, L. Xu, L.G.M. Pettersson, Water: A tale of two liquids, *Chem. Rev.* 116 (2016) 7463–7500.
- [10] J. Russo, K. Akahane, H. Tanaka, Water-like anomalies as a function of tetrahedrality, *Proc. Natl. Acad. Sci.* 115 (15) (2018) E3333–E3341.
- [11] P.G. Debenedetti, F. Sciortino, G.H. Zerze, Second critical point in two realistic models of water, *Science* 369 (2020) 289–292.
- [12] J. Palmer, F. Martelli, Y. Liu, R. Car, A.Z. Panagiotopoulos, P.G. Debenedetti, Metastable liquid–liquid transition in a molecular model of water, *Nature* 510 (2014) 385–388.
- [13] P. Gallo, F. Sciortino, Ising universality class for the liquid–liquid critical point of a one component fluid: A finite-size scaling test, *Phys. Rev. Lett.* 109 (2012) 177801.
- [14] V.M. Trejos, F. Gámez, A. Torres-Carbajal, A. Martínez-Borquez, Monte carlo simulations and perturbation theory for highly correlated fluids: The lennard-jones core softened potential case, *J. Mol. Liq.* 299 (2020) 112201.
- [15] P. Gallo, M. Rovere, D. Corradini, Ion hydration and structural properties of water in aqueous solutions at normal and supercooled conditions: a test of the structure making and breaking concept, *Phys. Chem. Chem. Phys.* 13 (2011) 19814–19822.
- [16] C. Zhang, S. Yue, A.Z. Panagiotopoulos, M.L. Klein, X. Wu, Dissolving salt is not equivalent to applying a pressure on water, *Nat. Commun.* 13 (2022) 822.
- [17] R. Mancinelli, A. Botti, F. Bruni, M.A. Ricci, A.K. Soper, Perturbation of water structure due to monovalent ions in solution, *Phys. Chem. Chem. Phys.* 9 (2007) 2959–2967.
- [18] J. Holzmann, R. Ludwig, A. Geiger, D. Paschek, Pressure and salt effects in simulated water: Two sides of the same coin?, *Angew Chem.* 46 (2007) 8907–8911.
- [19] Y. Marcus, Ionic radii in aqueous solutions, *Chem. Rev.* 88 (8) (1988) 1475–1498.
- [20] M.T.H. Nguyen, O. Tichacek, H. Martinez-Seara, P.E. Mason, P. Jungwirth, Resolving the equal number density puzzle: Molecular picture from simulations of  $\text{licl}(\text{aq})$  and  $\text{nacl}(\text{aq})$ , *J. Phys. Chem. B* 125 (2021) 3153–3162.
- [21] R. Mancinelli, A. Botti, F. Bruni, M.A. Ricci, A.K. Soper, Hydration of sodium, potassium, and chloride ions in solution and the concept of structure maker/breaker, *J. Phys. Chem. B* 111 (2007) 13570–13577.
- [22] B. Hribar, N.T. Southall, V. Vlachy, K.A. Dill, How ions affect the structure of water, *J. Am. Chem. Soc.* 124 (2002) 12302–12311.
- [23] I. Pethes, Towards the correct microscopic structure of aqueous  $\text{cscl}$  solutions with a comparison of classical interatomic potential models, *J. Molec. Liq.* 361 (2022) 119660.
- [24] S. Wang, J. Jacquemin, P. Husson, C. Hardacre, M.F. Costa Gomes, Liquid miscibility and volumetric properties of aqueous solutions of ionic liquids as a function of temperature, *J. Chem. Thermodyn.* 41 (11) (2009) 1206–1214.
- [25] M. Tariq, M. Esperança, M. Soromenho, L. Rebelo, J.C. Lopes, Shifts in the temperature of maximum density (tmd) of ionic liquid aqueous solutions, *Phys. Chem. Chem. Phys.* 15 (2013) 10960–10970.
- [26] G. Wada, S. Umeda, Effects of nonelectrolytes on the temperature of the maximum density of water. ii. organic compounds with polar groups, *Bull. Chem. Soc. Jpn.* 35 (1962) 1797–1801.
- [27] D. González-Salgado, J. Troncoso, E. Lomba, The temperature of maximum density for amino acid aqueous solutions. an experimental and molecular dynamics study, *Fluid Phase Equilib.* 521 (2020) 112703.
- [28] E.W. Washburn, *International Critical Tables of Numerical Data, Physics, Chemistry and Technology*, Vol. III, McGraw Hill, New York, 1928.
- [29] E.G. Pérez, D. González-Salgado, E. Lomba, Molecular dynamics simulations of aqueous solutions of short chain alcohols. excess properties and the temperature of maximum density, *Fluid Phase Equilib.* 528 (2021) 112840.
- [30] G. Wada, S. Umeda, Effects of nonelectrolytes on the temperature of the maximum density of water. i. alcohols, *Bull. Chem. Soc. Jpn.* 35 (1962) 646–652.
- [31] J. Troncoso, A new methodology for determining the temperature of maximum density against pressure. application to 2-propanol and ethanol aqueous solutions, *Fluid Ph. Equilibria* 549 (4) (2021) 113191.
- [32] D. Gonzalez-Salgado, J. Troncoso, E. Lomba, The increment of the temperature of maximum density of water by addition of small amounts of tert-butanol: Experimental data and microscopic description revisited, *J. Chem. Phys.* 156 (10) (2022) 104502.
- [33] M.C. Despretz *Ann. Chim. Phys.*, vol. 70, p. 49, 1839.
- [34] M.C. Despretz *Ann. Chim. Phys.*, vol. 73, p. 296, 1840.
- [35] L.C. Coppel, Ueber einige ältere bestimmungen des gefrierpunktes gesättigter salzlösungen, *Zeitschrift für Physikalische Chemie* 22U (1897) 239–240.
- [36] R. Wright, Xiii.–the effect of some simple electrolytes on the temperature of maximum density of water, *J. Chem Soc. Trans.* 115 (1919) 119–126.
- [37] T.H. Lilley, S. Murphy, The temperature of maximum density of aqueous electrolyte solutions and its relation to the temperature derivative of the partial molar volume of the solute, *J. Chem. Thermodyn.* 5 (1972) 467–470.
- [38] A.J. Darnell, J. Greyson, The effect of structure-making and -breaking solutes on the temperature of maximum density of water, *J. Phys. Chem.* 72 (1968) 3021–3025.
- [39] T. Wakabayashi, K. Takaizumi, Despretz constants for individual ions, *Bull. Chem. Soc. Jpn.* 55 (1982) 3073–3078.
- [40] M.V. Kaulgud, W.K. Pokale, Measurement of the temperature of maximum density of aqueous solutions of some salts and acids, *J. Chem. Soc., Faraday Trans.* 91 (1995) 999–1004.
- [41] W.K. Pokale, A.W. Pokale, Temperature of maximum density of water-electrolytes: A review, *Int. J. Chem. Phys. Sci.* 10 (2021) 10–26.
- [42] L.F. Sedano, S. Blazquez, E.G. Noya, C. Vega, J. Troncoso, Maximum in density of electrolyte solutions: Learning about ion-water interactions and testing the madrid-2019 force field, *J. Chem. Phys.* 156 (2022) 154502.
- [43] D. Corradini, M. Rovere, P. Gallo, Liquid–liquid coexistence in  $\text{nacl}$  aqueous solutions: A simulation study of concentration effects 115 (2011) 14161–14166.
- [44] M.P. Longinotti, M.A. Carignano, I. Szeleifer, H.R. Corti, Anomalies in supercooled  $\text{nacl}$  aqueous solutions: A microscopic perspective, *J. Chem. Phys.* 134 (2011) 244510.
- [45] T. Koop, L. Beiping, A. Tsias, T. Peter, Water activity as the determinant for homogeneous ice nucleation in aqueous solutions, *Nature* 406 (2000) 611–614.

- [46] A.W. Omta, M.F. Kropman, S. Woutersen, H.J. Bakker, Negligible effect of ions on the hydrogen-bond structure in liquid water, *Science* 301 (2003) 347–349.
- [47] K.J. Tielrooij, N. Garcia-Araez, M. Bonn, H.J. Bakker, Cooperativity in ion hydration, *Science* 328 (2010) 1006–1009.
- [48] E. Guàrdia, D. Laria, J. Martí, Hydrogen bond structure and dynamics in aqueous electrolytes at ambient and supercritical conditions, *J. Phys. Chem. B* 110 (2006) 6332–6338.
- [49] Y. Marcus, Effect of ions on the structure of water: Structure making and breaking, *Chem. Rev.* 109 (2009) 1346–1370.
- [50] I. Waluyo, C. Huang, D.N.U. Bergmann, T.M. Weiss, L.G.M. Pettersson, A. Nilsson, The structure of water in the hydration shell of cations from x-ray raman and small angle x-ray scattering measurements, *J. Chem. Phys.* 134 (2011) 064513.
- [51] J.R. Errington, P.G. Debenedetti, Relationship between structural order and the anomalies of liquid water, *Nature* 409 (2001) 318–321.
- [52] H. Ohtaki, T. Radnai, Structure and dynamics of hydrated ions, *Chem. Rev.* 3 (1993) 1157–1204.
- [53] H. Du, J. Rasaiah, J.D. Miller, Ions in water: characterizing the forces that control chemical processes and biological structure, *J. Phys. Chem. B* 111 (2007) 209.
- [54] H.S. Frank, W. Evans, Free volume and entropy in condensed systems iii. entropy in binary liquid mixtures; partial molal entropy in dilute solutions; structure and thermodynamics in aqueous electrolytes, *J. Chem. Phys.* 13 (1945) 507.
- [55] I. Waluyo, C. Huang, D. Nordlund, T.M. Weiss, L.G.M. Pettersson, A. Nilsson, Increased fraction of low-density structures in aqueous solutions of fluoride, *J. Chem. Phys.* 134 (2011) 224507.
- [56] H.S. Frank, A.L. Robinson, The entropy of dilution of strong electrolytes in aqueous solutions, *J. Chem. Phys.* 8 (1940) 933.
- [57] R.W. Gurney, *Ionic Processes in Solution*, McGraw Hill, New York, 1953.
- [58] J.S. Kim, W. Zhe, A.R. Morrow, A. Yethiraj, A. Yethiraj, Self-diffusion and viscosity in electrolyte solutions, *J. Phys. Chem.* 116 (2012) 12007–12013.
- [59] K. Collins, M.W. Washabaugh, The Hofmeister effect and the behaviour of water at interfaces, *Q. Rev. Biophys.* 18 (1985) 323–422.
- [60] M.W. Washabaugh, K. Collins, The systematic characterization by aqueous column chromatography of solutes which affect protein stability, *J. Bio. Chem.* 261 (1986) 12477–12485.
- [61] C.P. Lamas, C. Vega, E.G. Noya, Freezing point depression of salt aqueous solutions using the Madrid-2019 model, *J. Chem. Phys.* 156 (2022) 134503.
- [62] W.K. Pokale, M.V. Kaulgud, Correlating despretz constant with limiting partial molal expansibility, *Indian Journal of Chemistry* 33A (1994) 1008–1010.
- [63] I. Zeron, J.L.F. Abascal, C. Vega, A force field of  $\text{Li}^+$ ,  $\text{Na}^+$ ,  $\text{K}^+$ ,  $\text{Mg}^{2+}$ ,  $\text{Ca}^{2+}$ ,  $\text{Cl}^-$ , and  $\text{SO}_4^{2-}$  in aqueous solution based on the TIP4P/2005 water model and scaled charges for the ions, *J. Chem. Phys.* 151 (2019) 134504–134516.
- [64] S. Blazquez, M.M. Conde, J.L.F. Abascal, C. Vega, The Madrid-2019 force field for electrolytes in water using TIP4P/2005 and scaled charges: Extension to the ions  $\text{F}^-$ ,  $\text{Br}^-$ ,  $\text{I}^-$ ,  $\text{Rb}^+$ , and  $\text{Cs}^+$ , *J. Chem. Phys.* 156 (2022) 044505.
- [65] W.L. Jorgensen, J. Chandrasekhar, J.D. Madura, R.W. Impey, M.L. Klein, Comparison of simple potential functions for simulating liquid water, *J. Chem. Phys.* 79 (2) (1983) 926–935.
- [66] H.J.C. Berendsen, J.R. Grigera, T.P. Straatsma, The missing term in effective pair potentials, *J. Phys. Chem.* 91 (24) (1987) 6269–6271.
- [67] C. Vega, J.L.F. Abascal, Simulating water with rigid non-polarizable models: a general perspective, *Phys. Chem. Phys.* 13 (2011) 19663–19688.
- [68] H.W. Horn, W.C. Swope, J.W. Pitera, J.D. Madura, T.J. Dick, G.L. Hura, T. Head-Gordon, Development of an improved four-site water model for biomolecular simulations: Tip4p-ew, *J. Chem. Phys.* 120 (20) (2004) 9665–9678.
- [69] S. Pianna, A.G. Donchev, P. Robustelli, D.E. Shaw, Water dispersion interactions strongly influence simulated structural properties of disordered protein states, *J. Phys. Chem. B* 119 (16) (2015) 5113–5123.
- [70] J.L.F. Abascal, C. Vega, A general purpose model for the condensed phases of water: Tip4p/2005, *J. Chem. Phys.* 123 (2005) 234505.
- [71] J.L.F. Abascal, C. Vega, Note: Equation of state and compressibility of supercooled water: Simulations and experiment, *J. Chem. Phys.* 134 (2011) 186101.
- [72] I. Leontyev, A. Stuchebrukhov, Electronic continuum model for molecular dynamics simulations, *J. Chem. Phys.* 130 (8) (2009) 085103.
- [73] I.V. Leontyev, A.A. Stuchebrukhov, Electronic continuum model for molecular dynamics simulations of biological molecules, *J. Chem. Theory Comput.* 6 (2010) 1498–1508.
- [74] I.V. Leontyev, A.A. Stuchebrukhov, Electronic polarizability and the effective pair potentials of water, *J. Chem. Theory Comput.* 6 (2010) 3153–3161.
- [75] I.V. Leontyev, A.A. Stuchebrukhov, Accounting for electronic polarization in non-polarizable force fields, *Phys. Chem. Phys.* 13 (2011) 2613–2626.
- [76] I.V. Leontyev, A.A. Stuchebrukhov, Polarizable mean-field model of water for biological simulations with amber and charmm force fields, *J. Chem. Theory Comput.* 8 (9) (2012) 3207–3216.
- [77] I.V. Leontyev, A.A. Stuchebrukhov, Polarizable molecular interactions in condensed phase and their equivalent nonpolarizable models, *J. Chem. Phys.* 141 (1) (2014) 014103.
- [78] E. Pluhařová, P.E. Mason, P. Jungwirth, Ion pairing in aqueous lithium salt solutions with monovalent and divalent counter-anions, *J. Phys. Chem. A* 117 (46) (2013) 11766–11773.
- [79] M. Kohagen, P.E. Mason, P. Jungwirth, Accounting for electronic polarization effects in aqueous sodium chloride via molecular dynamics aided by neutron scattering, *J. Phys. Chem. B* 120 (8) (2015) 1454–1460.
- [80] S.W. Rick, S.J. Stuart, B.J. Berne, Dynamical fluctuating charge force-fields - application to liquid water, *J. Chem. Phys.* 101 (1994) 6141–6156.
- [81] M. Soniat, S.W. Rick, The effects of charge transfer on the aqueous solvation of ions, *J. Chem. Phys.* 137 (4) (2012) 044511.
- [82] Z. Kann, J. Skinner, A scaled-ionic-charge simulation model that reproduces enhanced and suppressed water diffusion in aqueous salt solutions, *J. Chem. Phys.* 141 (10) (2014) 104507.
- [83] A.J. Lee, S.W. Rick, The effects of charge transfer on the properties of liquid water, *J. Chem. Phys.* 134 (18) (2011) 184507.
- [84] M. Soniat, S.W. Rick, Charge transfer effects of ions at the liquid water/vapor interface, *J. Chem. Phys.* 140 (18) (2014) 184703.
- [85] M. Soniat, G. Pool, L. Franklin, S.W. Rick, Ion association in aqueous solution, *Fluid Phase Equilib.* 407 (2016) 31–38.
- [86] Y. Yao, M.L. Berkowitz, Y. Kanai, Communication: Modeling of concentration dependent water diffusivity in ionic solutions: Role of intermolecular charge transfer, *J. Chem. Phys.* 143 (2015) 241101.
- [87] M. Předota, D. Biriukov, Electronic continuum correction without scaled charges, *J. Molec. Liq.* 314 (2020) 113571.
- [88] C. Vega, Water one molecule, two surfaces, one mistake, *Mol. Phys.* 113 (2015) 1145.
- [89] D.E. Hare, C.M. Sorensen, The density of supercooled water. ii. bulk samples cooled to the homogeneous nucleation limit, *J. Chem. Phys.* 87 (1987) 4840.
- [90] M. Laliberte, W.E. Cooper, Model for calculating the density of aqueous electrolyte solutions, *J. Chem. Eng. Data* 49 (5) (2004) 1141–1151.
- [91] P. Novotný, O. Söhnel, Densities of binary aqueous solutions of 306 inorganic substances, *J. Chem. Eng. Data* 33 (1988) 49.
- [92] B. Hess, C. Kutzner, D. van der Spoel, E. Lindahl, Gromacs 4: Algorithms for highly efficient, load-balanced, and scalable molecular simulation, *J. Chem. Theory Comput.* 4 (2008) 435–447.
- [93] S. Nosé, A molecular dynamics method for simulations in the canonical ensemble, *Mol. Phys.* 52 (2) (1984) 255–268.
- [94] W.G. Hoover, Canonical dynamics: equilibrium phase-space distributions, *Phys. Rev. A* 31 (1985) 1695–1697.
- [95] M. Parrinello, A. Rahman, Polymorphic transitions in single crystals: A new Molecular Dynamics method, *J. Appl. Phys.* 52 (1981) 7182–7190.
- [96] D. Beeman, Some multistep methods for use in molecular dynamics calculations, *J. Comput. Phys.* 20 (2) (1976) 130–139.
- [97] U. Essmann, L. Perera, M.L. Berkowitz, T. Darden, H. Lee, L.G. Pedersen, A smooth particle mesh ewald method, *J. Chem. Phys.* 103 (1995) 8577–8593.
- [98] S. Blazquez, C. Vega, Melting points of water models: Current situation, *J. Chem. Phys.* 156 (21) (2022) 216101.
- [99] J. Kolafa, Pressure in molecular simulations with scaled charges. 1. ionic systems, *J. Phys. Chem. B* 124 (34) (2020) 7379–7390.
- [100] J.L. Fulton, G.K. Schenter, M.D. Baer, C.J. Mundy, L.X. Dang, M. Balasubramanian, Probing the hydration structure of polarizable halides: A multi-edge xafs and molecular dynamics study of the iodide anion, *J. Phys. Chem. B* 114 (2010) 12926–12937.
- [101] Y. Tamura, T. Yamaguchi, I. Okada, H. Ohtaki, An x-ray diffraction study on the structure of concentrated aqueous caesium iodide and lithium iodide solutions, *Zeitschrift für Naturforschung A* 42 (1987) 367–376.
- [102] H. Ohtaki, T. Radnai, Structure and dynamics of hydrated ions, *Chem. Rev.* 3 (1993) 1157–1204.
- [103] I. Kalcher, J. Dzubiella, Structure-thermodynamics relation of electrolyte solutions, *J. Chem. Phys.* 130 (2009) 134507.
- [104] A. Caruso, X. Zhu, J.L. Fulton, F. Paesani, Accurate modeling of bromide and iodide hydration with data-driven many-body potentials 126 (2022) 8266–8278.
- [105] D. Zhuang, M. Riera, G.K. Schenter, J.L. Fulton, F. Paesani, Many-body effects determine the local hydration structure of  $\text{cs}^+$  in solution, *J. Phys. Chem. Lett.* 10 (2019) 406–412.
- [106] J. Dočkal, M. Lísal, F. Moučka, Polarizable force fields for accurate molecular simulations of aqueous solutions of electrolytes, crystalline salts, and solubility:  $\text{Li}^+$ ,  $\text{Na}^+$ ,  $\text{K}^+$ ,  $\text{Rb}^+$ ,  $\text{F}^-$ ,  $\text{Cl}^-$ ,  $\text{Br}^-$ ,  $\text{I}^-$ , *J. Molec. Liq.* 362 (2022) 119659.
- [107] A.Z. Panagiotopoulos, Simulations of activities, solubilities, transport properties, and nucleation rates for aqueous electrolyte solutions, *J. Chem. Phys.* 153 (2020) 010903.
- [108] S. Deublein, J. Vrabec, H. Hasse, A set of molecular models for alkali and halide ions in aqueous solution, *J. Chem. Phys.* 136 (8) (2012) 084501.
- [109] M. Kohagen, P.E. Mason, P. Jungwirth, Accurate description of calcium solvation in concentrated aqueous solutions, *J. Phys. Chem. B* 118 (28) (2014) 7902–7909.
- [110] J. Kolafa, Solubility of nacl in water and its melting point by molecular dynamics in the slab geometry and a new bk3-compatible force field, *The Journal of chemical physics* 145 (20) (2016) 204509.
- [111] T. Yagasaki, M. Matsumoto, H. Tanaka, Lennard-jones parameters determined to reproduce the solubility of NaCl and KCl in SPC/E, TIP3P, and TIP4P/2005 water, *J. Chem. Theory Comput.* 16 (2020) 2460.
- [112] I.S. Joung, T.E. Cheatham, Determination of alkali and halide monovalent ion parameters for use in explicitly solvated biomolecular simulations, *J. Phys. Chem. B* 112 (2008) 9020–9041.
- [113] D.E. Smith, L.X. Dang, Computer simulations of nacl association in polarizable water, *J. Chem. Phys.* 100 (1994) 3757.
- [114] G.S. Kell, *J. Chem. Eng. Data* 20 (1968) 97–105.
- [115] R. Schmid, A. Miah, V. Sapunov, A new table of the thermodynamic quantities of ionic hydration: Values and some applications (enthalpy-entropy compensation and born radii), *Phys. Chem. Chem. Phys.* 2 (1) (2000) 97–102.

- [116] S. Blazquez, I.M. Zeron, M.M. Conde, J.L.F. Abascal, C. Vega, Scaled charges at work: Salting out and interfacial tension of methane with electrolyte solutions from computer simulations, *Fluid Phase Equilib.* 513 (2020) 112548.
- [117] D. Biriukov, H.-W. Wang, N. Rampal, C. Tempira, P. Kula, J.C. Neufeind, A.G. Stack, M. Pedota, The "good", the "bad" and the "hidden" in neutron scattering and molecular dynamics of ionic aqueous solutions, *J. Chem. Phys.* 156 (2022) 194505, <https://doi.org/10.1063/5.0093643>.
- [118] L. Åke Näslund, D.C. Edwards, P. Wernet, U. Bergmann, H. Ogasawara, L.G.M. Pettersson, S. Myneni, A. Nilsson, X-ray absorption spectroscopy study of the hydrogen bond network in the bulk water of aqueous solutions 109 (2005) 5995–6002.
- [119] M. Laliberté, *J. Chem. Eng. Data* 52 (2007) 321.
- [120] A.G. Ostroff, B.S.S. Jr, D.E. Woessner, Viscosities of protonated and deuterated water solutions of alkali metal chlorides, *J. Phys. Chem.* 73 (1969) 2784.
- [121] A. Benavides, M. Portillo, J. Abascal, C. Vega, Estimating the solubility of 1:1 electrolyte aqueous solutions: the chemical potential difference rule, *Mol. Phys.* 115 (9–12) (2017) 1301–1308.
- [122] W.M. Haynes, *CRC handbook of chemistry and physics*, CRC Press, 2011.
- [123] R. Okamoto, K. Koga, A. Onuki, Ion size dependences of the salting-out effect: Reversed order of sodium and lithium ions, *J. Phys. Chem.* 153 (2020) 074503.
- [124] K.D. Collins, Ions from the hofmeister series and osmolytes: effects on proteins in solution and in the crystallization process, *Methods* 34 (2004) 300–311.
- [125] C.D. Cappa, J.D. Smith, K.R. Wilson, B.M. Messer, M.K. Gilles, R.C. Cohen, R.J. Saykally, Effects of alkali metal halide salts on the hydrogen bond network of liquid water vol. 109 (2005) 7046.
- [126] C.D. Cappa, J.D. Smith, B.M. Messer, R.C. Cohen, R.J. Saykally, Effects of cations on the hydrogen bond network of liquid water: New results from x-ray absorption spectroscopy of liquid microjets vol. 110 (2006) 5301.
- [127] O.D. Bonner, C.F. Jumper, *Infrared Phys.* 13 (3) (1973) 233–242.
- [128] F. Hofmeister, Zur lehre von der wirkung der salze, *Arch Exp Pathol Pharmacol* 24 (1888) 247–260.
- [129] W. Kunz, J. Henle, B.W. Ninham, Zur lehre von der wirkung der salze: Franz hofmeister's historical papers, *Curr Opin Colloid Interface Sci* 9 (2004) 1937.
- [130] Y. Zhang, P.S. Cremer, Interactions between macromolecules and ions: the hofmeister series, *Current opinion in chemical biology* 10 (2006) 658–663.
- [131] H.I. Okur, H. Hladílková, K.B. Rembert, Y. Cho, J. Heyda, J. Dzubiella, P.S. Cremer, P. Jungwirth, "Beyond the hofmeister series: Ion-specific effects on proteins and their biological functions 121 (9) (2017) 1997–2014.
- [132] S. Yue, A.Z. Panagiotopoulos, Dynamic properties of aqueous electrolyte solutions from non-polarisable, polarisable, and scaled-charge models, *Mol. Phys.* 117 (23–24) (2019) 3538–3549, <https://doi.org/10.1063/5.0093643>.